

Hence,

$$dh + u du = 0 \quad (5.10)$$

To reinforce the comments made at the beginning of this section, we emphasize that Eqs. (5.1), (5.2), (5.5), (5.7), (5.9), and (5.10) are *exact* representations of physics as applied to the *approximate* model of quasi-one-dimensional flow. So the basic fundamental physical principles stated in Chap. 2 are not compromised here. The only compromise with the true nature of the flow is the use of the simplified *model* of quasi-one-dimensional flow.

Return to the roadmap in Fig. 5.5. We have completed the left column, and we are now ready to use the fundamental governing equations for quasi-one-dimensional flow to study the properties of nozzle and diffuser flows. However, before going to these applications, we move to the right side of the roadmap and obtain the area-velocity relation. This relation is vital to understanding the *physics of the flow*, and we need this understanding before we go to the applications.

## 5.3 | AREA-VELOCITY RELATION

A wealth of physical information regarding quasi-one-dimensional flow can be obtained from a particular combination of the differential forms of the conservation equations presented at the end of Sec. 5.2 as shown next. From Eq. (5.7),

$$\frac{d\rho}{\rho} + \frac{du}{u} + \frac{dA}{A} = 0 \quad (5.11)$$

To eliminate  $d\rho/\rho$  from Eq. (5.11), consider Eq. (5.9):

$$\frac{dp}{\rho} = \frac{dp}{d\rho} \frac{d\rho}{\rho} = -u du \quad (5.12)$$

Recall that we are considering adiabatic, inviscid flow, i.e., there are no dissipative mechanisms such as friction, thermal conduction, or diffusion acting on the flow. Thus, the flow is isentropic. Hence, any change in pressure,  $dp$ , in the flow is accompanied by a corresponding isentropic change in density,  $d\rho$ . Therefore, we can write

$$\frac{dp}{d\rho} = \left( \frac{\partial p}{\partial \rho} \right)_s = a^2 \quad (5.13)$$

Combining Eqs. (5.12) and (5.13),

$$a^2 \frac{d\rho}{\rho} = -u du$$

or

$$\frac{d\rho}{\rho} = -\frac{u du}{a^2} = -\frac{u^2 du}{a^2 u} = -M^2 \frac{du}{u} \quad (5.14)$$

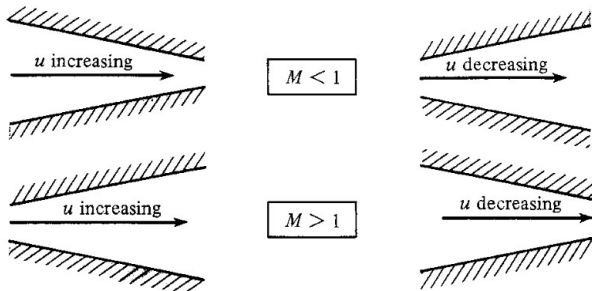


**Figure 5.8 |** Flow in converging and diverging ducts.

Substituting Eq. (5.14) into Eq. (5.11),

$$\boxed{\frac{dA}{A} = (M^2 - 1) \frac{du}{u}} \quad (5.15)$$

Equation (5.15) is an important result. It is called the *area-velocity relation*, and it tells us this information:

1. For  $M \rightarrow 0$ , which in the limit corresponds to incompressible flow, Eq. (5.15) shows that  $Au = \text{const}$ . This is the familiar continuity equation for incompressible flow.
2. For  $0 \leq M < 1$  (subsonic flow), an *increase* in velocity (positive  $du$ ) is associated with a *decrease* in area (negative  $dA$ ), and vice versa. Therefore, the familiar result from incompressible flow that the velocity increases in a converging duct and decreases in a diverging duct still holds true for subsonic compressible flow (see top of Fig. 5.8).
3. For  $M > 1$  (supersonic flow), an *increase* in velocity is associated with an *increase* in area, and vice versa. Hence, we have a striking difference in comparison to subsonic flow. For supersonic flow, the velocity increases in a diverging duct and decreases in a converging duct (see bottom of Fig. 5.8).
4. For  $M = 1$  (sonic flow), Eq. (5.15) yields  $dA/A = 0$ , which mathematically corresponds to a minimum or maximum in the area distribution. The minimum in area is the only physically realistic solution, as described next.

These results clearly show that for a gas to expand isentropically from subsonic to supersonic speeds, it must flow through a convergent-divergent duct (or streamtube), as sketched at the top of Fig. 5.9. Moreover, at the minimum area that divides the convergent and divergent sections of the duct, we know from item 4 above that the flow must be sonic. This minimum area is called a *throat*. Conversely, for a gas to compress isentropically from supersonic to subsonic speeds, it must also flow through a convergent-divergent duct, with a throat where sonic flow occurs, as sketched at the bottom of Fig. 5.9.

From this discussion, we recognize why rocket engines have large, bell-like nozzle shapes as sketched in Fig. 5.10—to expand the exhaust gases to high-velocity,

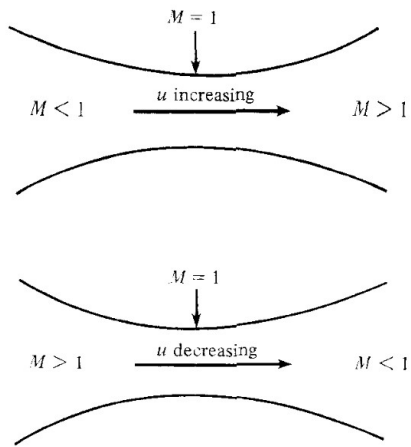


**Figure 5.9** | Flow in a convergent-divergent duct.

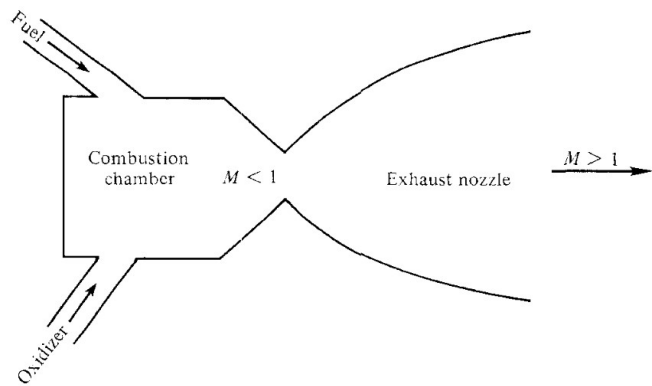


**Figure 5.10** | Schematic of a rocket engine.

supersonic speeds. This bell-like shape is clearly evident in the photograph of the space shuttle main engine shown in Fig. 5.3. Moreover, we can infer the configuration of a supersonic wind tunnel, which is designed to first expand a stagnant gas to supersonic speeds for aerodynamic testing, and then compress the supersonic stream back to a low-speed subsonic flow before exhausting it to the atmosphere. This general configuration is illustrated in Fig. 5.11. Stagnant gas is taken from a reservoir and expanded to high subsonic velocities in the convergent portion of the nozzle. At the minimum area (the first throat), sonic flow is achieved. Downstream of the throat, the flow goes supersonic in the divergent portion of the nozzle. At the end of the nozzle, designed to achieve a specified Mach number, the supersonic flow enters the test section, where a test model or other experimental device is usually situated. Downstream of the test section, the supersonic flow enters a diffuser, where it is slowed down in a convergent duct to sonic flow at the second throat, and then further slowed to low subsonic speeds in a divergent duct, finally being exhausted to the atmosphere.

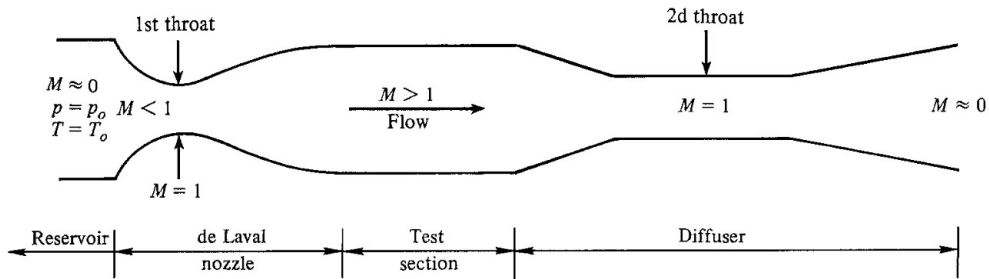


**Figure 5.11 |** Schematic of a supersonic wind tunnel.

This discussion, along with Fig. 5.11, is a simplistic view of real supersonic wind tunnels, but it serves to illustrate the basic phenomena as revealed by the area-velocity relation, Eq. (5.15). Also note that a convergent-divergent nozzle is sometimes called a *de Laval* (or *Laval*) nozzle, after Carl G. P. de Laval, who first used such a configuration in his steam turbines in the late nineteenth century, as described in Secs. 1.1 and 5.8.

The derivation of Eq. (5.15) utilized only the basic conservation equations—no assumption as to the type of gas was made. Hence, Eq. (5.15) is a general relation which holds for real gases and chemically reacting gases, as well as for a perfect gas—as long as the flow is isentropic. We will visit this matter again in Chap. 17.

The area-velocity relation is a differential relation, and in order to make quantitative use of it, we need to integrate Eq. (5.15). However, there is a more direct way of obtaining quantitative relations for quasi-one-dimensional flow, which we will see in the next section. The primary importance of the area-velocity relation is the invaluable *physical* information it provides, as we have already discussed.

We now move to the bottom of our roadmap in Fig. 5.5. Using the fundamental governing equations as well as the physical information provided by the area-velocity relation, we examine the first of the two central applications in this chapter—flows through nozzles.

## 5.4 | NOZZLES

The analysis of flows through variable-area ducts in a general sense requires numerical solutions such as those to be discussed in Chap. 17. However, based on our experience obtained in Chaps. 3 and 4, we suspect (correctly) that we can obtain closed-form results for the case of a calorically perfect gas. We will divide our discussion into two parts: (1) purely isentropic subsonic-supersonic flow through nozzles and (2) the effect of different pressure ratios across nozzles.

### 5.4.1 Isentropic Subsonic-Supersonic Flow of a Perfect Gas through Nozzles

Consider the duct shown in Fig. 5.12. At the throat, the flow is sonic. Hence, denoting conditions at sonic speed by an asterisk, we have, at the throat,  $M^* = 1$  and

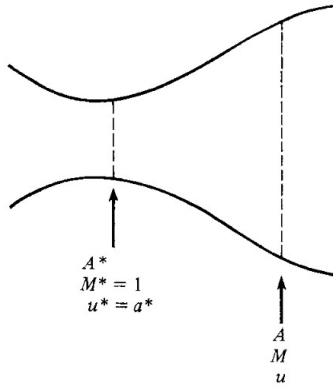


**Figure 5.12** | Geometry for derivation of the area Mach number relation.

$u^* = a^*$ . The area of the throat is  $A^*$ . At any other section of the duct, the local area, Mach number, and velocity are  $A$ ,  $M$ , and  $u$ , respectively. Apply Eq. (5.1) between these two locations:

$$\rho^* u^* A^* = \rho u A \quad (5.16)$$

Since  $u^* = a^*$ , Eq. (5.16) becomes

$$\frac{A}{A^*} = \frac{\rho^* a^*}{\rho u} = \frac{\rho^* \rho_o a^*}{\rho_o \rho u} \quad (5.17)$$

where  $\rho_o$  is the stagnation density defined in Sec. 3.4, and is constant throughout the isentropic flow. Repeating Eq. (3.31),

$$\frac{\rho_o}{\rho} = \left( 1 + \frac{\gamma - 1}{2} M^2 \right)^{1/(\gamma-1)}$$

and apply this to sonic conditions, we have

$$\frac{\rho_o}{\rho^*} = \left( \frac{\gamma + 1}{2} \right)^{1/(\gamma-1)} \quad (5.18)$$

Also, by definition, and from Eq. (3.37),

$$\left( \frac{u}{a^*} \right)^2 = M^{*2} = \frac{\frac{\gamma + 1}{2} M^2}{1 + \frac{\gamma - 1}{2} M^2} \quad (5.19)$$

Squaring Eq. (5.17), and substituting Eqs. (3.31), (5.18), and (5.19), we have

$$\begin{aligned}\left(\frac{A}{A^*}\right)^2 &= \left(\frac{\rho^*}{\rho_o}\right)^2 \left(\frac{\rho_o}{\rho}\right)^2 \left(\frac{a^*}{u}\right)^2 \\ \left(\frac{A}{A^*}\right)^2 &= \left(\frac{2}{\gamma+1}\right)^{2/(\gamma-1)} \left(1 + \frac{\gamma-1}{2} M^2\right)^{2/(\gamma-1)} \left(\frac{1 + \frac{\gamma-1}{2} M^2}{\frac{\gamma+1}{2} M^2}\right) \\ \boxed{\left(\frac{A}{A^*}\right)^2 = \frac{1}{M^2} \left[\frac{2}{\gamma+1} \left(1 + \frac{\gamma-1}{2} M^2\right)\right]^{(\gamma+1)/(\gamma-1)}} \quad (5.20)\end{aligned}$$

Equation (5.20) is called the *area-Mach number relation*, and it contains a striking result. Turned inside out, Eq. (5.20) tells us that  $M = f(A/A^*)$ , i.e., the Mach number at any location in the duct is a function of the ratio of the local duct area to the sonic throat area. As seen from Eq. (5.15),  $A$  must be greater than or at least equal to  $A^*$ ; the case where  $A < A^*$  is physically not possible in an isentropic flow. Also, from Eq. (5.20) there are two values of  $M$  that correspond to a given  $A/A^* > 1$ , a subsonic and a supersonic value. The solution of Eq. (5.20) is plotted in Fig. 5.13,

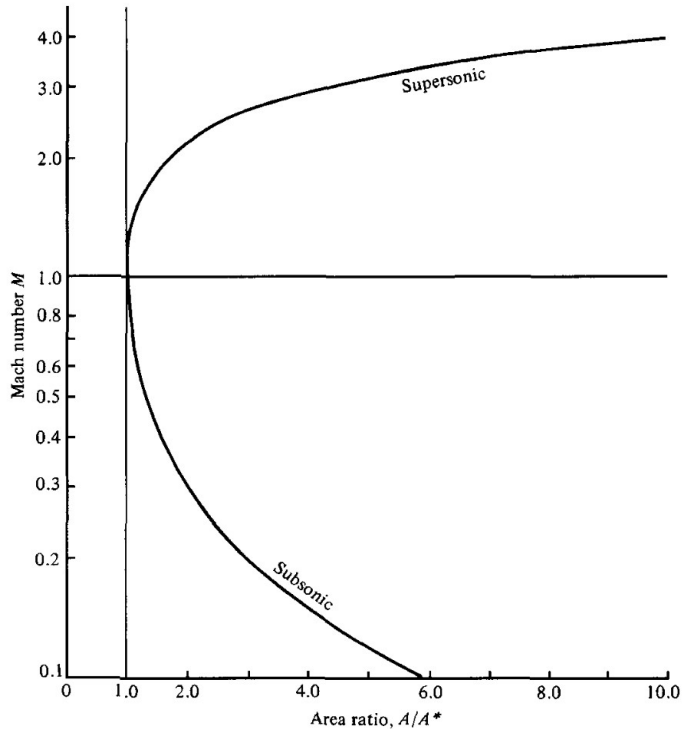


**Figure 5.13 | Area-Mach number relation.**

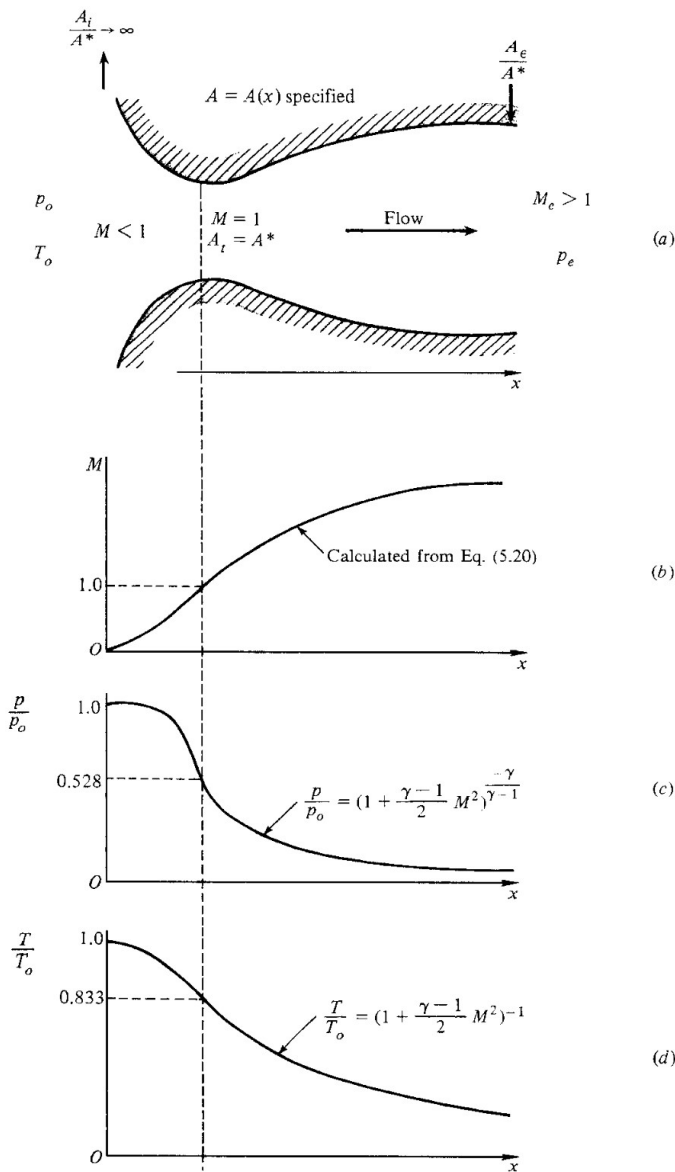


**Figure 5.14** | Isentropic supersonic nozzle flow.

which clearly delineates the subsonic and supersonic branches. Values of  $A/A^*$  as a function of  $M$  are tabulated in Table A.1 for both subsonic and supersonic flow.

Consider a given convergent-divergent nozzle, as sketched in Fig. 5.14a. Assume that the area ratio at the inlet  $A_i/A^*$  is very large,  $A_i/A^* \rightarrow \infty$ , and that the inlet is fed with gas from a large reservoir at pressure and temperature  $p_o$  and  $T_o$ , respectively. Because of the large inlet area ratio,  $M \approx 0$ ; hence  $p_o$  and  $T_o$  are essentially stagnation (or total) values. (The Mach number cannot be precisely zero in the reservoir,

or else there would be no mass flow through the nozzle. It is a finite value, but small enough to assume that it is *essentially* zero.) Furthermore, assume that the given convergent-divergent nozzle expands the flow isentropically to supersonic speeds at the exit. For the given nozzle, there is only *one* possible isentropic solution for supersonic flow, and Eq. (5.20) is the key to this solution. In the convergent portion of the nozzle, the subsonic flow is accelerated, with the subsonic value of  $M$  dictated by the local value of  $A/A^*$  as given by the lower branch of Fig. 5.13. The consequent variation of Mach number with distance  $x$  along the nozzle is sketched in Fig. 5.14b. At the throat, where the throat area  $A_t = A^*$ ,  $M = 1$ . In the divergent portion of the nozzle, the flow expands supersonically, with the supersonic value of  $M$  dictated by the local value of  $A/A^*$  as given by the upper branch of Fig. 5.13. This variation of  $M$  with  $x$  in the divergent nozzle is also sketched in Fig. 5.14b. Once the variation of Mach number through the nozzle is known, the variations of static temperature, pressure, and density follow from Eqs. (3.28), (3.30), and (3.31), respectively. The resulting variations of  $p$  and  $T$  are shown in Figs. 5.14c and d, respectively. Note that the pressure, density, and temperature decrease continuously throughout the nozzle. Also note that the exit pressure, density, and temperature ratios,  $p_e/p_o$ ,  $\rho_e/\rho_o$ , and  $T_e/T_o$  depend only on the exit area ratio,  $A_e/A^*$  via Eq. (5.20). If the nozzle is part of a supersonic wind tunnel, then the test section conditions are completely determined by  $A_e/A^*$  (a geometrical design condition) and  $p_o$  and  $T_o$  (gas properties in the reservoir).

#### 5.4.2 The Effect of Different Pressure Ratios Across a Given Nozzle

If a convergent-divergent nozzle is simply placed on a table, and nothing else is done, obviously nothing is going to happen; the air is not going to start rushing through the nozzle of its own accord. To accelerate a gas, a pressure difference must be exerted, as clearly stated by Euler's equation, Eq. (5.9). Therefore, in order to establish a flow through any duct, the exit pressure must be lower than the inlet pressure, i.e.,  $p_e/p_o < 1$ . Indeed, for completely shockfree isentropic supersonic flow to exist in the nozzle of Fig. 5.14a, the exit pressure ratio must be precisely the value of  $p_e/p_o$  shown in Fig. 5.14c.

What happens when  $p_e/p_o$  is *not* the precise value as dictated by Fig. 5.14c? In other words, what happens when the backpressure downstream of the nozzle exit is independently governed (say by exhausting into an infinite reservoir with controllable pressure)? Consider a convergent-divergent nozzle as sketched in Fig. 5.15a. Assume that no flow exists in the nozzle, hence  $p_e = p_o$ . Now assume that  $p_e$  is minutely reduced below  $p_o$ . This small pressure difference will cause a small wind to blow through the duct at low subsonic speeds. The local Mach number will increase slightly through the convergent portion of the nozzle, reaching a maximum at the throat, as shown by curve 1 of Fig. 5.15b. This maximum will *not* be sonic; indeed it will be a low subsonic value. Keep in mind that the value  $A^*$  defined earlier is the *sonic* throat area, i.e., that area where  $M = 1$ . In the case we are now considering, where  $M < 1$  at the minimum-area section of the duct, the real throat area of the duct,  $A_t$ , is larger than  $A^*$ , which for completely subsonic flow takes on the

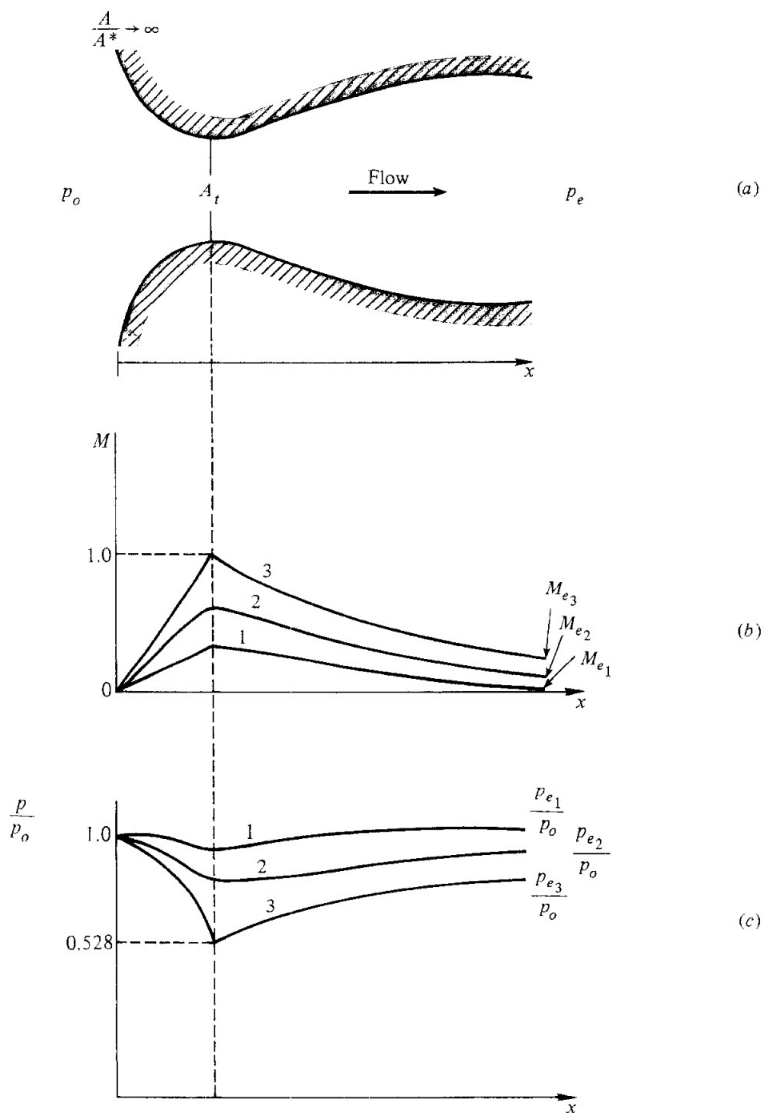


**Figure 5.15** | Subsonic flow in a convergent-divergent nozzle.

character of a reference quantity different from the actual geometric throat area. Downstream of the throat, the subsonic flow encounters a diverging duct, and hence  $M$  decreases as shown in Fig. 5.15b. The corresponding variation of static pressure is given by curve 1 in Fig. 5.15c. Now assume  $p_e$  is further reduced. This stronger pressure ratio between the inlet and exit will now accelerate the flow more, and the variations of subsonic Mach number and static pressure through the duct will be larger, as indicated by curve 2 in Figs. 5.15b and c. If  $p_e$  is further reduced, there will be

some value of  $p_e$  at which the flow will just barely go sonic at the throat, as given by the curve 3 in Figs. 5.15b and c. In this case,  $A_t = A^*$ . Note that all the cases sketched in Figs 5.15b and c are subsonic flows. Hence, for *subsonic* flow through the convergent-divergent nozzle shown in Fig. 5.15a, there are an *infinite number of isentropic solutions*, where both  $p_e/p_o$  and  $A/A_t$  are the controlling factors for the local flow properties at any given section. This is a direct contrast with the supersonic case discussed in Sec. 5.4.1, where only *one* isentropic solution exists for a given duct, and where  $A/A^*$  becomes the only controlling factor for the local flow properties (relative to reservoir properties).

For the cases shown in Figs. 5.15a, b, and c, the mass flow through the duct increases as  $p_e$  decreases. This mass flow can be calculated by evaluating Eq. (5.1) at the throat,  $\dot{m} = \rho_t A_t u_t$ . When  $p_e$  is reduced to  $p_{e_3}$ , where sonic flow is attained at the throat, then  $\dot{m} = \rho^* A^* a^*$ . If  $p_e$  is now reduced further,  $p_e < p_{e_3}$ , the Mach number at the throat cannot increase beyond  $M = 1$ ; this is dictated by Eq. (5.15). Hence, the flow properties at the throat, and indeed throughout the entire subsonic section of the duct, become “frozen” when  $p_e < p_{e_3}$ , i.e., the subsonic flow becomes unaffected and the mass flow remains constant for  $p_e < p_{e_3}$ . This condition, after sonic flow is attained at the throat, is called *choked flow*. No matter how low  $p_e$  is made, after the flow becomes choked, the mass flow remains constant. This phenomenon is illustrated in Fig. 5.16. Note from Eq. (3.35) that sonic flow at the throat corresponds to a pressure ratio  $p^*/p_o = 0.528$  for  $\gamma = 1.4$ ; however, because of the divergent duct downstream of the throat, the value of  $p_{e_3}/p_o$  required to attain sonic flow at the throat is larger than 0.528, as shown in Figs. 5.15c and 5.16.

What happens in the duct when  $p_e$  is reduced below  $p_{e_3}$ ? In the convergent portion, as we stated, nothing happens. The flow properties remain as given by the subsonic portion of curve 3 in Fig. 5.15b and c. However, a lot happens in the divergent portion of the duct. No isentropic solution is allowed in the divergent duct until  $p_e$  is adequately reduced to the specified low value dictated by Fig. 5.14c. For values of exit pressure above this, but below  $p_{e_3}$ , a normal shock wave exists inside the divergent duct. This situation is sketched in Fig. 5.17. Let the exit pressure be given by  $p_{e_4}$ . There is a region of supersonic flow ahead of the shock. Behind the

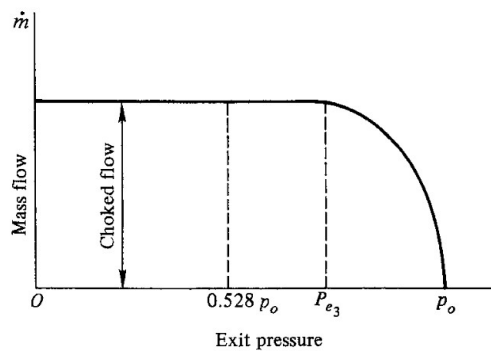


**Figure 5.16 |** Variation of mass flow with exit pressure; illustration of choked flow.

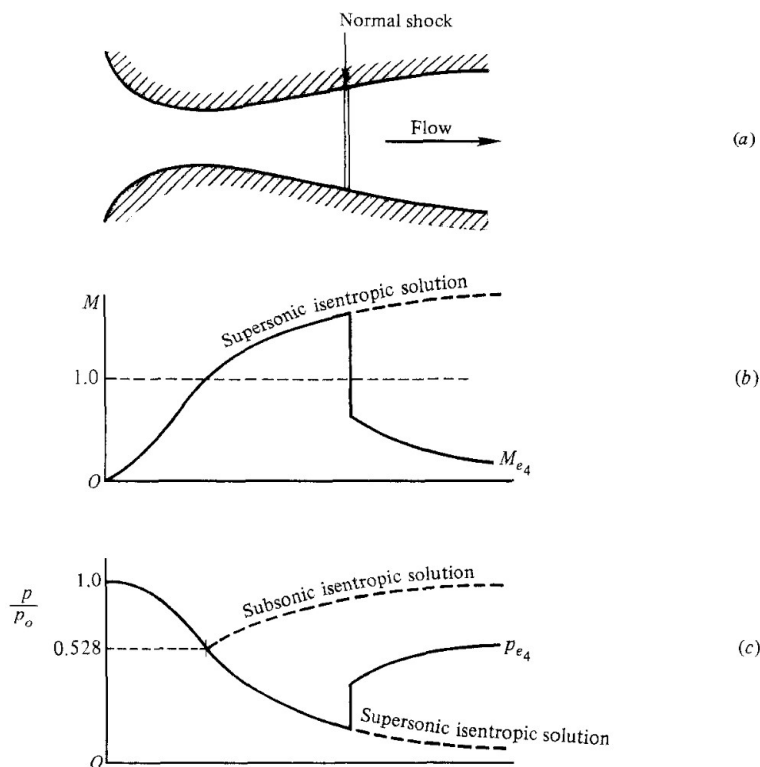


**Figure 5.17 |** Flow with a shock wave inside a convergent-divergent nozzle.

shock, the flow is subsonic, hence the Mach number decreases towards the exit and the static pressure increases to  $p_{e_4}$  at the exit. The location of the normal shock wave in the duct is determined by the requirement that the increase of static pressure across the wave plus that in the divergent portion of the subsonic flow behind the shock be just right to achieve  $p_{e_4}$  at the exit. As the exit pressure is reduced further, the normal shock wave will move downstream, closer to the nozzle exit. It will stand precisely at the exit when  $p_e = p_{e_5}$ , where  $p_{e_5}$  is the static pressure behind a normal shock at the design Mach number of the nozzle. This is illustrated in Figs. 5.18a, b, and c. In Fig. 5.18c,  $p_{e_6}$  represents the proper isentropic value for the design exit Mach number, which exists immediately upstream of the normal shock wave standing at the exit. When the downstream backpressure  $p_B$  is further decreased such that  $p_{e_6} < p_B < p_{e_5}$ , the flow inside the nozzle is fully supersonic and isentropic, with the behavior the same as given earlier in Figs. 5.14 a, b, c, and d. The increase to the backpressure takes place across an oblique shock attached to the nozzle exit, but outside the duct itself. This is sketched in Fig. 5.18d. If the backpressure is further reduced below  $p_{e_6}$ , equilibration of the flow takes place across expansion waves outside the duct, as shown in Fig. 5.18e.

When the situation in Fig. 5.18d exists, the nozzle is said to be *overexpanded*, because the pressure at the exit has expanded below the back pressure,  $p_{e_6} < p_B$ .

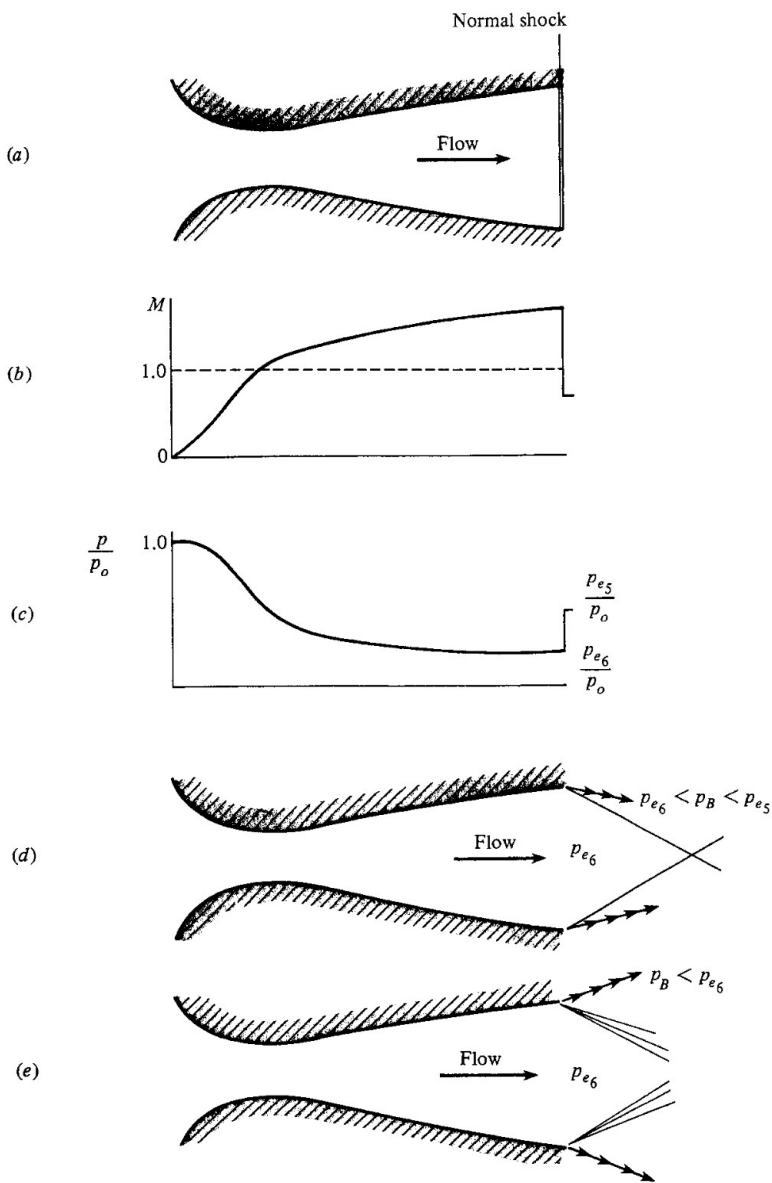


**Figure 5.18** | Flow with shock and expansion waves at the exit of a convergent-divergent nozzle.

Conversely, when the situation in Fig. 5.18e exists, the nozzle is said to be *underexpanded*, because the exit pressure is higher than the back pressure,  $p_{e6} > p_B$ , and hence the flow is capable of additional expansion after leaving the nozzle.

The results of this section are particularly important and useful. The reader should make certain to reread this section until he or she feels comfortable with the concepts and results before proceeding further. Also, keep in mind that these

quasi-one-dimensional considerations allow the analysis of cross-sectional averaged properties inside a nozzle of given shape. They do not tell us much about how to design the *contour* of a nozzle—especially that for a supersonic nozzle in order to ensure shockfree, isentropic flow. If the shape of the walls of a supersonic nozzle is not just right, oblique shock waves can occur inside the nozzle. The proper contour for a supersonic nozzle can be determined from the method of characteristics, to be discussed in Chap. 11.

**EXAMPLE 5.1**

Consider the isentropic subsonic-supersonic flow through a convergent-divergent nozzle. The reservoir pressure and temperature are 10 atm and 300 K, respectively. There are two locations in the nozzle where  $A/A^* = 6$ : one in the convergent section and the other in the divergent section. At each location, calculate  $M$ ,  $p$ ,  $T$ , and  $u$ .

**Solution**

In the *convergent* section, the flow is subsonic. From the front of Table A.1, for subsonic flow with  $A/A^* = 6$ :  $M = 0.097$ ,  $p_o/p = 1.006$ , and  $T_o/T = 1.002$ . Hence

$$\begin{aligned} p &= \frac{p}{p_o} p_o = (1.006)^{-1}(10) = 9.94 \text{ atm} \\ T &= \frac{T}{T_o} T_o = (1.002)^{-1}(300) = 299.4 \text{ K} \\ a &= \sqrt{\gamma RT} = \sqrt{(1.4)(287)(299.4)} = 346.8 \text{ m/s} \\ u &= Ma = (0.097)(346.8) = 33.6 \text{ m/s} \end{aligned}$$

In the *divergent* section, the flow is supersonic. From the supersonic section of Table A.1, for  $A/A^* = 6$ :  $M = 3.368$ ,  $p_o/p = 63.13$ , and  $T_o/T = 3.269$ . Hence

$$\begin{aligned} p &= \frac{p}{p_o} p_o = (63.13)^{-1}(10) = 0.1584 \text{ atm} \\ T &= \frac{T}{T_o} T_o = (3.269)^{-1}(300) = 91.77 \text{ K} \\ a &= \sqrt{\gamma RT} = \sqrt{(1.4)(287)(91.77)} = 192.0 \text{ m/s} \\ u &= Ma = (3.368)(192.0) = 646.7 \text{ m/s} \end{aligned}$$

**EXAMPLE 5.2**

A supersonic wind tunnel is designed to produce Mach 2.5 flow in the test section with standard sea level conditions. Calculate the exit area ratio and reservoir conditions necessary to achieve these design conditions.

**Solution**

From Table A.1, for  $M_e = 2.5$ :

$$A_e/A^* = 2.637 \quad p_o/p_e = 17.09 \quad T_o/T_e = 2.25$$